Volume 1

The Long-Baseline Neutrino Experiment (LBNE)

May 10, 2010 DRAFT

NOTE: Most figures in this draft are placeholders

Contents

Acronyms, Abbreviations and Definitions

A	Amps
AC	Alternating Current
Access	Database program from Microsoft Corporation
ACOE	Army CORP of Engineers
ACWP	Actual Cost of Work Performed
ADC	Analog-to-Digital Converter
AGS	Alternate Gradient Synchrotron
ALD	Associate Laboratory Director
AP	Antiproton
APS	American Physical Society
ASHRAE	American Society of Heating, Refrigerating and Air Conditioning Engineers
ATLAS	A Toroidal LHC Apparatus
BAC	Budget at Completion
BCP	Baseline Change Proposal
BCWP	Budgeted Cost for Work Performed
BCWS	Budgeted Cost for Work Scheduled
BNL	Brookhaven National Laboratory
BO	Beneficial Occupancy
CAIRS	Computerized Accident Incident Recordkeeping and Reporting System
CAM	Control Account Manager
CC	Charged-Current Neutrino Interactions
CCB	Change Control Board
CCD	Charge-Coupled Device
CD	Computing Division
CD-0	Critical Decision-0
CD-1	Critical Decision-1
CD-2	Critical Decision-2
CD-3	Critical Decision-3
CD-4	Critical Decision-4
CDR	Conceptual Design Report
CERN	European Organization for Nuclear Research
cfm	Cubic feet per minute
C.L.	Confidence Level
COE	Army CORP of ENgineers
CP	Charge-Parity Symmetry
CPT	Charge-Parity Time Reversal Symmetry
DAC	Digital-to-Analog Converter
DAQ	Data Acquisition
DC	Direct Current
DCR	Document Change Request
DocDB	Document Data Base
DOE	Department of Energy
DPM	Deputy Project Manager
DUSEL	Deep Underground Science and Engineering Laboratory
DWS	Domestic Water Service
EA	Environmental Assessment
EAC	Estimates at Completion
EDIA	Engineering, Design, Inspection, Administration

ED&I	Engineering, Design and Inspection
EENF	Environmental Evaluation Form
ES	Elastic Neutrino Scattering
ES&H	Environment, Safety and Health
FADC	Flash Analog-to-Digital Converter
FEA	Finite Element Analysis
FEC	Front-End Card
FEE	Front-End Electronics
FEMA	Federal Emergency Management Agency
Fermilab	Fermi National Accelerator Laboratory
FESHM	Fermilab ES&H Manual
FESS	Facilities Engineering Services Section (at Fermilab)
FET	Field Effect Transistor
FNAL	Fermi National Accelerator Laboratory
FONSI	Finding of No Significant Impact
FPD	Federal Project Director
FPGA	Field Programmable Gate Array
FRA	Fermi Research Alliance, LLC
FSS	Facility Safety Systems
ft	Feet
FWHM	Full Width at Half Maximum
FY	Fiscal Year
GEANT	Geometry and Tracking simulation software
gpm	Gallons per minute
GPS	Global Positioning System
HEP	High Energy Physics
HND	Homestake Neutrino Detector
HS	Highway Standard
HV	High Voltage
HVAC	Heating Ventilating and Air Conditioning
ICS	Integrated Cost/Schedule
ICW	Industrial Cooling Water
ISM	Integrated Safety Management
ISO	International Standards of Organization
IQA	Integrated Quality Assurance (program at Fermilab)
JTAG	Joint Test Action Group
K2K	KEK to Kamiokande Neutrino Oscillation Experiment
KamLAND	Kamioka Liquid Scintillator Antineutrino Detector
KEK	High Energy Accelerator Research Organization in Japan
KRS	Kautz Road Substation
kV	Kilo (1,000) volts
kVA	Kilo (1,000) volt amps (or kilowatt, electrical power)
kw	Kilowatt
L1	Level 1
L2	Level 2
L3	Level 3
L4	Level 4
LabVIEW	Laboratory Virtual Instrument Engineering Workbench
LAr20	Liquid Argon Detector
LArTPC	Liquid Argon Time Projection Chamber
LBNE	Long-Baseline Neutrino Experiment
LBNE-PM	Long-Baseline Neutrino Experiment Project Manager
LBNE-PO	Long-Baseline Neutrino Experiment Project Office
LBNL	Lawrence Berkeley National Laboratory
LCW	Low Conductivity Water

LED	Light Emitting Diode
LEED	Leadership for Energy Efficient Design
Lf	Lineal feet
LMA	Large Mixing Angle solution
LSND	Liquid Scintillator Neutrino Detector
LVDS	Low Voltage Differential
MBLT	Multiplexed Block Transfer
MC	Monte Carlo
MEP	Mechanical, Electrical and Plumbing
MI	Main Injector
MIE	Major Item of Equipment
MINOS	Main Injector Neutrino Oscillation Experiment
ML	Maximum Liklihood
MOU	Memorandum of Understanding
MR	Management Reserve
m.w.e.	Meters of Water Equivalent
NC	Neutral Current Neutrino Interactions
NEPA	National Environmental Protection Act
NFPA	National Fire Protection Association
NSS	Near Surface Storage (Facility)
NSF	National Science Foundation
NTP	Network Time Protocol
NuSAG	Neutrino Science Assessment Group
ODH	Oxygen Deficiency Hazard
OPC	Other Project Costs
OPMO	Office of Project Management and Oversight
ORPS	Occurrence Reporting and Processing System
P5	Particle Physics Project Prioritization Panel
PA	Photomultiplier tube Assembly
PAP	Project Advisory Panel
PC	Personal Computer
PDR	Project Definition Report
p.e.	Photo-Electrons
PEP	Project Execution Plan
P-PEP	Preliminary Project Execution Plan
PIR	Panel of Institutional Representatives
PIU	Photomultiplier tube Installation Unit
PLL	Phase-Locked Loop
PM	Project Manager
PMCS	Project Management Control System
PMG	Project Management Group
PMP	Project Management Plan
PMT	Photomultiplier Tube
PPD	Particle Physics Division
PSAD	Preliminary Safety Assessment Document
PSL	Physical Sciences Laboratory at the University of Wisconsin
PVC	Poly Vinyl Chloride
QA	Quality Assurance
QAP	Quality Assurance Plan
QC	Quality Control
QE	Quantum Efficiency
QM	Quality Management
R&D	Research and Development
RACF	RHIC and ATLAS Computing Facility
RAW	Radioactive Water

RHIC	Relativistic Heavy Ion Collider
RLS	Resource Loaded Schedule
RPVC	Rigid Poly Vinyl Chloride
RQD	Rock Quality Designation
RS	Richter Scale
SAD	Safety Assessment Document
SBMS	Standards Based Management System
SDSTA	South Dakota Science and Technology Administration
SF	Square Feet
SM	System Manager
SNO	Sudbury Neutrino Observatory
SNO+	Proposed solar and geo-neutrino experiment using liquid scintillator in SNO detector
SOW	Statement of Work
s.p.e.	Single Photon-Electron
SS	Stainless Steel
SSO	Senior Safety Officer
Sta.	Station (100 ft, distance increment, e.g., Sta. 1+00 = 100 ft)
SUSEL	Stanford Underground Science and Engineering Laboratory
SV	Schedule Variance
TB	Technical Board
TDC	Time-to-Digital Converter
TDR	Technical Design Report
TPC	Time Projection Chamber
TPC	Total Project Cost
UCT	Universal Coordinated Time
UV	Ultraviolet light
VAC	Variance at Completion
VME	Versa Module Europa
WBS	Work Breakdown Structure
WCD	Water Cherenkov Detector
WCD-PM	Water Cherenkov Detector Project Management
WCD-PO	Water Cherenkov Detector Project Office

List of Figures

[Will generate later after all figures are in and numbered]

List of Tables

[Will generate later after all tables are in and numbered]

1 Executive Summary

1.1 Introduction

The Long-Baseline Neutrino Experiment (LBNE) Project Team has prepared this Conceptual Design Report for a world-class facility that will enable the scientific community to carry out a compelling research program in neutrino physics. The ultimate goal in the operation of the facility and experimental program is to measure fundamental physical parameters, explore physics beyond the Standard Model and better elucidate the nature of matter and antimatter.

Although the Standard Model of particle physics presents a remarkably accurate description of the elementary particles and their interactions, we know that the current model is incomplete and that a more fundamental underlying theory must exist. Results from the last decade revealing that the three known types of neutrinos have nonzero mass, mix with one another and oscillate between generations point to physics beyond the Standard Model. Measuring the mass and other properties of neutrinos is fundamental to understanding the deeper underlying theory and will profoundly shape our understanding of the evolution of the universe.

In its 2008 report, the Particle Physics Project Prioritization Panel (P5) recommended a world-class neutrino physics program as a core component of the U.S. particle physics program. Included in the report is the long-term vision of a large detector in the proposed Deep Underground Science and Engineering Laboratory (DUSEL) and a high-intensity neutrino source at Fermi National Accelerator Laboratory (FNAL). On January 8, 2010, the Department of Energy approved the Mission Need for a new long-baseline neutrino experiment that would enable this world-class program and firmly establish the U.S. as the leader in neutrino science. The LBNE Project is being designed to meet this Mission Need.

With the facilities provided by the LBNE Project, the LBNE Science Collaboration would be able to make unprecedentedly precise measurements of neutrino oscillation parameters, including the value of the third mixing angle and the sign of the neutrino mass hierarchy. The ultimate goal of the program will be to search for CP-violation in the neutrino sector. The preferred configuration of the LBNE facility, in which a large neutrino detector is located deep underground, could also provide opportunities for research in other areas of physics, such as nucleon decay and neutrino astrophysics.

1.2 Scope

The LBNE project scope includes construction of a facility comprised of a large detector illuminated by a distant, intense neutrino source and a much smaller detector located close to the source. The favored alternative for achieving the project's mission is to aim neutrinos, produced by protons from the Fermilab Main Injector, towards the NSF proposed DUSEL site at the Homestake Mine in Lead, South Dakota, located 1300 km from Fermilab. This configuration is the

basis for the design presented in this Conceptual Design Report. Specifically, the main scope elements include:

- A proton beam aimed at the far detector site
- A neutrino beam aimed at the far detector site
- A near detector complex located near the neutrino source
- Massive neutrino detectors located at the far detector site

1.3 Capabilities

Elements of the LBNE Project are being designed to optimize the measurement of neutrino oscillations, in particular electron neutrino appearance at the far detector. The main performance characteristics of the major project elements are given in Table 1. Detailed performance characteristics are presented in the respective volumes of the sub-projects.

1.4 Costs and Schedule

The Total Estimated Cost (TEC) of the LBNE Project is $XXX.X M. The Total Project Cost (TPC) is $YYY.Y M, which includes an NSF contribution of $ZZZ.Z M. The schedule for construction will lead to a start of operations in FY20??.

1.5 Acquisition Strategy

[This is a placeholder. Text will be developed based on the actual Acquisition Strategy that is developed by the Integrated Project Team (DOE + LBNE Project)]

The acquisition strategy relies on Fermi Research Alliance (FRA), the Department of Energy Managing and Operating (M&O) contractor for Fermi National Accelerator Laboratory, to directly manage the elements of the LBNE Project. This will include design, construction, fabrication, assembly, installation and pre-commissioning of project elements that will be located on the Fermilab site, as well as those at the far detector site, for which the Department of Energy is the steward.

Project Element	Performance Parameter

Table 1.1 To be completed : [!! Sub-project contributors should submit candidate elements to be included in this high level summary.]

2 The LBNE Project Overview

2.1 Project Mission

The primary mission of the LBNE Project is to construct facilities that will enable a search for $\nu_\mu \rightarrow \nu_e$ appearance over a distance (baseline) of greater than 1000 km. The magnitude of this signal is governed by the yet-to-be measured mixing angel, θ_{13}. Precise measurement of this phenomena would allow for determination of the relative masses and mass ordering of the three known neutrinos. Measurement of this neutrino oscillation channel would also allow for research into CP violation in the neutrino sector, which is possibly connected to the dominance of matter over antimatter in the universe.

To achieve precise neutrino oscillation measurements of this type requires an intense neutrino beam and detectors of unprecedented size. Such detectors, if located underground and thus shielded from the products of cosmic ray interactions, could also provide an opportunity for increased science, including the search for proton decay and observation of neutrinos generated by supernovae. In short, the LBNE project mission is to build an experimental facility in order to further our knowledge of neutrinos and work toward the discovery of new physics.

2.2 Project Scope

2.2.1 Overview

The LBNE project will be comprised of an intense neutrino source pointing toward a distant large detector and a much smaller detector located close to the source. The far detector must be a long distance from the neutrino source to increase sensitivity to neutrino oscillations. A nearby detector close to the neutrino source is necessary to measure the initial composition of the beam.

LBNE's targeted scope is to build a neutrino facility that uses a proton beam to produce a beam of neutrinos directed towards near and far detectors. There are two favored technologies being explored for the far detector – water Cherenkov and liquid argon. Water Cherenkov detectors have been successfully operated underground at a number of sites for more than twenty years [WC], whereas, large liquid argon detectors are a newer technology, requiring continued development to determine their cost and effectiveness [LAr]. The liquid argon detectors offer a potential advantage over water Cherenkov detectors in that the same performance may be achieved in a smaller detector due to higher efficiency[1]. For LBNE, two 100-kT Water-Cherenkov-Equivalent (WCE) cavern/detector ensembles are being considered for the far detector.

[1] Studies indicate that a 20kT (total volume) liquid argon detector may have equivalent capability to a 120 kT (total volume) water Cherenkov detector for ν_e detection efficiency and background rejection. [Dirk]

The preferred alternative for the neutrino source and near detector site is FNAL, as it has already developed the expertise for construction of neutrino beams as part of the NuMI/MINOS project. The 700-kW upgrade of the FNAL proton source, a component of the current NOvA project [NOvA], offers a platform from which to launch a new neutrino beam for a long-baseline detector. The proposed NSF Deep Underground Science and Engineering Laboratory (DUSEL) [DUSEL] site at Homestake Mine in Lead, South Dakota is the preferred alternative for the far detector site because it offers both sufficient depth for shielding from cosmic rays and an optimum distance of 1290 km from FNAL to detect neutrino oscillations.

2.2.2 Neutrino Beam Configuration

The key elements that define the neutrino beam configuration include the primary beam magnets, which transport the proton beam from the FNAL Main Injector and focus it onto a neutrino production target; magnetic horns, which focus pions produced at the target into a decay channel; and an absorber to stop the transport of un-interacted protons and hadrons that have not decayed.

The primary beam transport consists of dipole, quadrupole and corrector magnets, as well as vacuum, water and instrumentation control systems. The primary transport elements are configured such that at the location of the target, the beam is aimed at a downward angle of 5.6 degrees, or 10% slope, in the direction of the Homestake Mine. The remainder of the facility and components are constructed or installed in a manner to maintain this angle for the direction of the neutrino beam.

The primary proton beam will interact in a graphite target of approximately one meter length, which, for normal operation of LBNE, is inserted into the first of two magnetic horns used to focus the pions produced in the target. The Target Hall houses the targets, horns, radiation shielding and equipment for handling the components. Following the Target Hall will be a decay pipe, 4 m in diameter and 250 m in length, surrounded by between 3 to 4 meters of concrete shielding. An absorber will be installed following the decay tunnel, and a beam position monitor will be installed behind the absorber. The reference design for the neutrino beam is described in Volume 2 of this Conceptual Design Report.

2.2.3 Near Detector Configuration

Four hundred and twenty meters downstream of the end of the Absorber Hall an enclosure for the Near Detector(s) will be constructed. This enclosure will be approximately 110 meters below the earth's surface. Detectors which will measure the characteristics of the neutrino beam will be installed in this hall. Because the neutrino flux at this location is large, the size of the detectors is small (relative to the far detectors). A complex of small detectors with different technologies and capabilities offers the best opportunity to fully characterize the beam to the precision needed for normalization of the far detector observations. Options for the near detector complex include :

- Option 1 , mass = ?
- Option 2, mass = ?

- Option….

[This section will be completed after the outline of Volume 3 is submitted.]

2.2.4 Far Detector Configurations

[This section will be re-written after Volumes 4 and 5 are complete and a decision on how to present the far detector configurations has been made. For the May – June time frame, this section will present the configuration options that are being considered.]

As noted above, two different detector technologies are being pursued for the design of the far detector – water Cherenkov and liquid argon.

While originally conceived for proton decay searches, large water Cherenkov detectors have been constructed and demonstrated to be a cost-effective detector for neutrinos as well. The Super-Kamiokande II detector in Japan is a 50-kT total volume detector that has provided definitive measurements of solar and atmospheric neutrino parameters. It is currently the far detector for the JPARC [JPARC] neutrino beam program in pursuit of the measurement of the θ_{13} mixing angle [T2K]. Scaling the total mass of a water detector by a factor of two or three, though challenging, is deemed technically feasible.

The largest liquid argon detector to operate to date is the 300-ton module of the ICARUS detector, which had a brief commissioning run in a surface laboratory in 200? [ICARUS]. Currently, the two 300-ton ICARUS modules are being filled in the Gran Sasso Laboratory and will soon be capable of detecting neutrinos from the CNGS neutrino beam from CERN [CNGS]. An integrated plan for liquid argon detectors has been underway at Fermilab for several years, and the design of a 20-kT module for an LBNE detector is a key component of this plan [LArPlan].

In Chapter 3, the issue of the depth requirements for the far detector is discussed in some detail. Given the configuration of the underground spaces at the Homestake Mine, it is an obvious conclusion that a water Cherenkov detector should be located on the main DUSEL campus at 4850 ft. The situation is not so clear for a liquid argon detector, and during the conceptual design phase both deep and shallow options have been developed.

The far detector configurations that have been developed during the LBNE post-CD-0 conceptual design phase are summarized in Table 2.1

Configuration	WCD @ 4850 ft	LAr @ 4830 ft	LAr @ 300 or 800 ft
a	2 x 100 kT		
b		2 x 20 kT	
c			2 x 20 kT
d	1 x 100 kT	1 x 20 kT	
e	1 x 100 kT		1 x 20 kT

Table 2.1 Five configurations being evaluated for the LBNE far detector configuration. 1 or 2 indicates the number of modules of the specified mass that would be placed at that depth.

2.2.5 Conventional Facilities

The LBNE Project is responsible for the design and construction of conventional facilities at both the Fermilab site and at the DUSEL site.

2.2.5.1 Conventional Facilities at Fermilab

The conventional facilities at Fermilab include the site preparation, surface service buildings, access shafts and underground enclosures required to transport the primary proton beam, produce the neutrino beam and house the near detectors for monitoring the neutrino beam. The Conceptual Design for these facilities is in Volume 6 of this CDR.

2.2.5.2 Conventional Facilities at DUSEL

The conventional facilities at DUSEL include the underground caverns required for the far detectors as well as the underground infrastructure associated with and required to support these caverns. It also includes surface buildings and infrastructure to support the detectors which will be installed in the caverns. These facilities have been designed in conjunction with the design of the DUSEL facility. Detailed conceptual design of the facilities and infrastructure required for the LBNE are presented as Volume 7 of this CDR.

2.3 Project Organization

The LBNE Project consists of five sub-projects, coordinated by a central project office located at FNAL:

1. The LBNE Neutrino Beamline
2. The LBNE Near Detectors
3. A Water Cherenkov Detector for LBNE
4. A Liquid Argon Detector for LBNE
5. Conventional Facilities

The FNAL project office is headed by the project manager and assisted by the project engineer and project scientist. Project office support staff include a chief financial officer, a lead project controls specialist, a documentation team and administrative support. The Neutrino Beamline, Liquid Argon and Conventional Facilities sub-projects are managed out of the FNAL project office, while the Near Detectors and Water Cherenkov sub-projects are managed out of project offices at Los Alamos National Laboratory and Brookhaven National Laboratory, respectively.

The LBNE project office has developed overriding plans for project management, risk management, configuration control and quality assurance [PM]. The sub-projects have developed

individually tailored plans as appropriate, and these are integrated into the overriding plans by reference and appendices.

A project organization chart is shown in Figure 2.1.
[This figure should be the same as generated for the PMP and other Project Documents.]

2.4 Work Breakdown Structure

The LBNE Project Work Breakdown Structure to level 4 is shown in Figure 2.2

2.5 Cost and Schedule

[This section is a placeholder]. It will be configured correctly once we decide how the far detector configuration will be presented.]

A preliminary high-level summary of the cost of the LBNE Project, at the second level of the work breakdown structure, is given in Table 2.2.

LBNE Level 2 Cost Element	Cost (FY10) ?? or AY??
1.1 Project Management	
1.2 Neutrino Beam	
1.3 Near Detector	
1.4 Water Cherenkov Far Detector	
1.5 Liquid Argon Far Detector	
1.6.1 Conventional Facilities at Fermilab	
1.6.2 Conventional Facilities at DUSEL	
LBNE Total Project Cost	

Table 2.2 Level 2/3 Cost Breakout for the LBNE Project

A preliminary Level 0 Milestone Schedule to construct the LBNE Project is shown in Table 2.3

Major Milestone Events	Preliminary Schedule
CD-0 (Approve Mission Need)	2nd Quarter 2010
CD-1 (Approve Alternative Selection and Cost Range)	2nd Quarter 2011
CD-2 (Approve Performance Baseline)	?? Quarter 2013
CD-3 (Approve Start of Construction)	?? Quarter 2014
CD-4 (Approve Start of Operations)	?? Quarter 2020

Table 2.3

References

[WC] IMB, Kamiokande, SuperK

[LAr] "Recommendations to the Department of Energy and the National Science Foundation on a Future US Program in Neutrino Oscillations – Report to the Nuclear Science Advisory Committee and the High Energy Physics Advisory Panel", Submitted by the Neutrino Scientific Assessment Group, July 13, 2007 http://www.er.doe.gov/hep/files/pdfs/NUSAGFinalReportJuly13,2007.pdf,

"US Particle Physics: Scientific Opportunities – A Strategic Plan for the Next Ten Years; Report of the Particle Physics Project Prioritization Panel, May 29, 2008, http://www.er.doe.gov/hep/files/pdfs/P5_Report%2006022008.pdf

[Dirk] Mark D. talk at UDiG

[NOvA] NOvA TDR

[DUSEL]

[JPARC]

[T2K]

[ICARUS]

[CNGS]

[LArPLAN]

[PM] Project Documents

3 Science With LBNE

[Note : This chapter is not meant to be a Proposal for science that one might hope to do with new detectors. It is to be a chapter which describes the science that the CDR detector configurations are capable of doing. It can, however, with appropriate introduction and clarification, describe science that could potentially be achieved with other "configurations" of detectors. Initially we will present and describe the science that is consistent with the 5 detector configurations in Table 2.1. We will modify this Chapter as the detector configurations become clearer.]

3.1 Overview

Particle physics has been very successful in creating a major synthesis of its findings, the Standard Model. At successive generations of particle accelerators in the U.S., Europe and Asia, physicists have used high-energy collisions to discover many new particles and make precision measurements of fundamental parameters. Simultaneously, scientists have carried out experiments to study naturally produced particles, such as the particles resulting from ultra-high-energy cosmic ray interactions and low-energy neutrinos emerging from the core of the sun. These efforts have uncovered both new principles and many unsuspected features of nature, resulting in an ever-increasing understanding of the workings of the universe.

In the past two decades, scientists have observed muon neutrinos produced in cosmic ray reactions in the Earth's atmosphere and electron neutrinos produced in nuclear reactions in the sun's core change from one flavor to another between source and detection. Further experimentation with both natural neutrino sources and neutrinos from reactors and accelerators has confirmed that the neutrino flavor states do not remain constant in time, but rather oscillate with a frequency governed by the magnitude of the differences between the three mass states of neutrinos.

As the name implies, the primary science motivation for the LBNE project is to study the phenomena of accelerator-generated long-baseline neutrino oscillations. A detailed description of this experiment is presented in Section 3.4. To carry out this experiment, LBNE requires construction of very large detectors, with masses of tens to hundreds of kilotons, depending on the specific technology of the detector. Locating these massive detectors deep underground, where they are shielded from backgrounds from cosmic ray interactions, provides the opportunity to extend the science goals to include searches for proton decay, neutrinos from supernovae, the sun, atmosphere and other rare phenomena.

The ability to have a broad range of physics capability has precedence in the history of underground detectors. Experimental programs initially implemented to search for proton decay have so far realized two significant successes in neutrino physics. The IMB [IMB] and Kamiokande [Kk] collaborations made an extremely impressive accidental discovery of supernova neutrinos in 1987, confirming the theory of supernova collapse. Subsequently, the physics program with Super-Kamiokande has been key to understanding solar and atmospheric neutrinos, including the definitive determination that neutrino oscillations explained the atmospheric neutrino anomaly [SK].

In the following sections, we describe the experimental searches that can be explored in the proposed LBNE detectors. These descriptions include the physics motivation, historical context and detector requirements to carry out each element of this program. Following the discussion of Accelerator Neutrino Oscillations in Section 3.4, Section 3.5 describes the means and methods for a next-generation search for proton decay. Section 3.6 describes the LBNE detectors capability to detect a supernova burst occurring in or near our galaxy. Section 3.7 proposes the means of possibly detecting the never-before-seen relic neutrinos from ancient and distant supernovae. [Note – as we gather requirements, we may end up combining burst and relic supernova neutrinos.] Section 3.8 describes a program of short-baseline physics that could be undertaken with the near detector complex described in Volume 3.

Section 3.9 discusses measurements that could be made with atmospheric and solar neutrinos, including possible determination of the neutrino mass hierarchy and the solar MSW day-night effect. This section also describes studies that could be undertaken to explore possible further exploitation of the LBNE detectors to include searches for more challenging or rare phenomena such as geo, reactor and ultra-high-energy neutrinos.

[Note for CDR development phase: this chapter includes placeholders for descriptions of the science case for each of the Topical Working Groups that has been set up. These sections will be developed as the Working Groups produce requirements and capabilities. The early drafts of this chapter will be based on text from previous studies and reports, but will be updated as a better analysis of the detector capabilities is produced. **Contributions and corrections welcome!!**]

3.2 Detector Technologies for LBNE

3.2.1 Overview

[In this section we want to describe the interactions that the detectors need to be able to detect, i.e. CC, NE, elastic scattering, inverse beta decay, etc. Describe the broad spectrum of energies that this program covers; all programs require large mass and good energy resolution. Summarize how the detector performance is a function of its depth (table from the depth document). Warn that low energy thresholds impose the need for enhancement of the detector, (i.e. gadolinium to enhance neutron capture, high phototube coverage and Q.E.,…) Introduce the general types of background that will be encountered, i.e. from NCπ^0 in beam physics to spallation backgrounds for low energy measurements…]

3.2.2 Water Cherenkov Detectors

The basic components of a water Cherenkov detector include a vessel to contain a large volume of water, which is the target material, and photomultiplier tubes (PMTs) lining the inner surface of the vessel to detect photons emitted by charged particles as they travel through the water. The charged particles result from interactions of neutrinos with the constituents of the water molecules, or from background particles entering or being created in the detector. When these

charged particles pass through the water with velocity greater than the speed of light in water[2], photons, called Cherenkov photons[3], are emitted in a cone around the direction of the particle's path. The emission angle for Cherenkov photons is given by:

$$\theta_c = \frac{1}{\beta n \lambda}$$

where β is the particle's velocity with respect to *c*, and λ is the wavelength of the Cherenkov light. While Cherenkov photons are emitted with a continuum of wavelengths, PMTs have a specific narrow range of wavelengths over which they are sensitive. For relativistic particles (β~1), nearly pure water (n~1.33) and λ~ ?nm, the Cherenkov angle is $\theta_c = 42^0$. Again for β~1, several hundred photons per centimeter of travel will be generated in the wavelength range of PMT sensitivity.

As the Cherenkov photons travel through the water and arrive at the vessel wall, the conical nature of the emission leads to a pattern of rings detectable by the array of PMTs. Signals from the PMTs are readout with electronics consisting of charge-to-digital converters and time-to-digital converters. The PMT readouts are then used to analyze the arrival time and number of photons in a ring. From this information, the direction, origin and energy of the original track can be reconstructed.

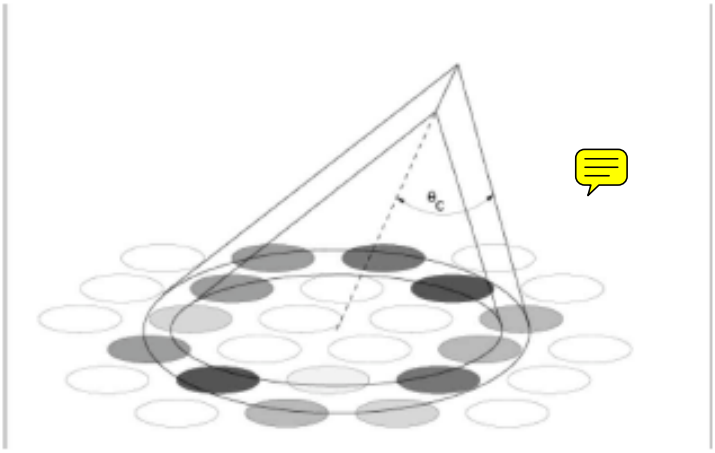

Figure 3.1 The Cherenkov light generated by the charged particle's path inside the detector arrives at the detector wall, where it produces a ring pattern that can be used to reconstruct the track's geometry and energy.

The direction, energy and flavor of a neutrino, ν, producing a charged-current neutrino interaction,

$$\nu_l + N \rightarrow l^- + X$$

[2] v > c/n, where c is the speed of light in vacuum and n is the index of refraction of water
[3] Historical context

within the detector volume may be reconstructed by measuring the direction, energy and flavor of the lepton, l. In a water Cherenkov detector muons can be distinguished from electrons by the pattern of light recorded by the PMTs. Because muons undergo very little scattering as they pass through the water, the ring pattern has a very "neat" outer edge. In contrast, particles such as electrons and photons will undergo multiple scattering and showering as they travel, producing a very ragged edge to the pattern of light in the PMTs. Figure 3.2 shows these distinct muon and electron patterns for two events in the Super-Kamiokande detector. [Note – this figure could/should be replaced with LBNE MC events.]

[Add overview/summary discussion of signal detection efficiency, energy resolution and backgrounds. Assume this is fully described in a detector performance chapter of Volume 4.]

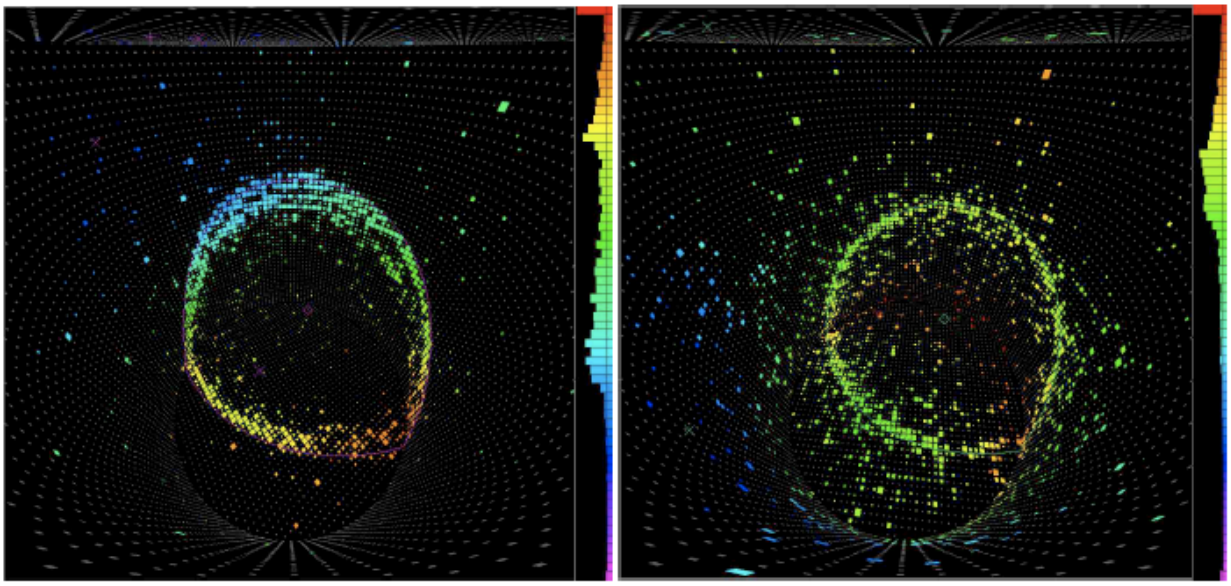

Figure 3.2 Two events displayed for the Super-Kamiokande detector. Left – muon, right – electron. To be replaced or supplemented by LBNE MC events

3.2.3 Liquid Argon Detectors

The basic components of a liquid argon detector include a cryostat, sets of cathode and anode planes, and readout electronics. The cryostat contains and maintains the liquid argon target material at a cryogenic temperature of 87^0 K. The sets of cathode and anode planes create a uniform electric field within the volume. The readout electronics on the anode planes record the passing charge of the ionization electrons created as charged particles drift through the liquid argon along the direction of the electric field. Figure 3.3 is an illustration of the basic idea. The set of planes is collectively called a Time Projection Chamber (TPC). The typical configuration of the anode wire planes is a set of two or three planes with 3 – 5 mm wire spacing, each separated by a few millimeters. The cathode plane is generally constructed of a solid conducting material. The cathode – anode separation sets the drift distance and is set by the achievable purity which governs the electron drift time. The wires are oriented with significant stereo angles with respect to each other. The first and second of the three planes are non-destructive to the passing charge and record the

charge by induction, and are therefore called induction planes. The final readout plane collects the charge from which the energy deposition can be determined, and is termed the collection plane. In addition to recording the induced or collected charge, the time of the arrival of the charge (relative to a t = 0 time stamp) is also recorded. By plotting the arrival time of a "hit" versus the wire numbers, a two-dimensional image of the event topology is created. Combining the hits from multiple views allows one to construct three-dimensional tracks and hence a three dimensional image of the event. The energy deposition from the collection plane is displayed in the varying intensity of the displayed tracks. As an example, a display of the raw data from interactions in the ArgoNeuT detector[4] are shown in Figure 3.4.

The topology of the tracks and the dE/dx along the track can be used to determine the type of event and its properties. For example, a cosmic ray muon will be reconstructed in the detector as a clear incoming track, whereas a neutrino interaction will create tracks that originate inside the chamber. Single electrons from the charged current interactions of ν_e can be differentiated from π^0 gamma rays by event topology and energy deposition in the first few centimeters of the event vertex.

[Add overview/summary discussion of signal detection efficiency, energy resolution and backgrounds.]

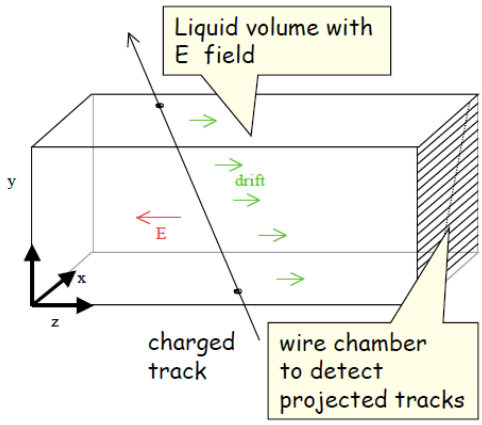

Figure 3.3 Schematic illustration of the basic principle of liquid argon detector [Need to make over following LBNE geometry…]

[4] ArgoNeuT is a 0.3-ton LArTPC which collected neutrino interactions in the NuMI beam in 2008. See reference xx.

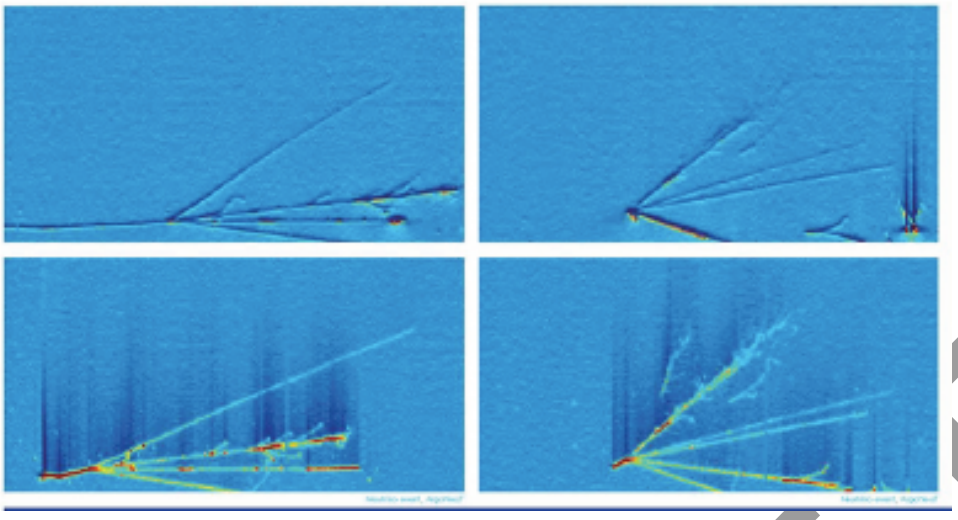

Figure 3.4 Neutrino interactions in the ArgoNeut detector (PLACEHOLDER)

3.3 Detector Depth Requirements

In 2008 the LBNE Science Collaboration undertook a detailed study of the depth requirements for the main signatures interest with large detectors. This work is referred to as "The Depth Document" [depth]. The topics considered were accelerator generated neutrinos, supernova, solar and atmospheric neutrinos and nucleon decay.

[Include a brief summary of the major issues and conclusions for each of the major topics.]

Table 3.1 summarizes the results of these studies for both a water Cherenkov and liquid argon[5] detector. It should be noted that none of these signatures requires a depth greater than the 4850 foot (4300 mwe) level at Homestake.

Physics	Water	Argon
Long-Baseline Accelerator	1,000	0-1,000
$p \rightarrow K^{+}\nu$	>3,000	>3,000
Day/Night ^{8}B Solar ν	,300	~4,300
Supernova Burst	3,500	3,500
Relic supernova	4,300	>2,500
Atmospheric ν	2,400	2,400

Table 3.1 The depth requirements in meters-water-equivalent (mwe) for different physics measurements and the two technologies being considered. This table is reproduced from Reference [depth].

[5] In the depth report it was assumed that there was no veto in the detector system. Inclusion of a veto may allow for operation at a shallower depth.

3.4 Accelerator Neutrino Oscillations

3.4.1 Historical Context

The concept of neutrino oscillations was first put forward by Bruno Pontecorvo in 1957, considering the possibility of $\nu \rightarrow \bar{\nu}$ oscillations [BP]. Neutrino oscillations imply that neutrinos have small masses and mix between states. In 1981 Kayser [BK] presented a description of the oscillations which will occur if the neutrino flavor states, ν_a and ν_b are linear combinations of the neutrino mass eignestates, ν_1 and ν_2. It can be shown that under a two neutrino hypothesis the probability of neutrino flavor change, for a neutrino of energy E and detected a distance L form the source, is given by :

$$P(\nu_a \rightarrow \nu_b) = \sin^2 2\theta_{12} \sin^2 (1.27 \Delta m^2_{12} \frac{L}{E})$$

In 1998 the Super-Kamiokande Collaboration announced "Evidence for Oscillation of Atmospheric Neutrinos" based on the observation of a deficit of muon neutrinos as a function of the distance traversed through the earth. The data were consistent with two-flavor $\nu_\mu \rightarrow \nu_\tau$ oscillations with $\sin^2 2\theta > 0.82$ and $5\times10^{-4} < \Delta m^2 < 6\times10^{-3}$ at 90% confidence level. This result, along with the decades long observation of a solar neutrino deficit and subsequent results from the SNO experiment, lead to the solid conclusion that neutrino oscillations had indeed been observed, and in fact with two distinct Δm^2. The KamLAND experiment confirmed oscillations at the "solar" mass difference via $\bar{\nu}_e$ disappearance from reactors. The K2K and MINOS accelerator long-baseline experiments confirmed the oscillation phenomena at the "atmospheric" mass difference via ν_μ-disappearance. ~~The on-going OPERA experiment in Gran Sasso, using the CNGS neutrino beam is attempting to measure oscillations in the $\nu_\mu \rightarrow \nu_\tau$ appearance channel.~~

3.4.2 Three Neutrino Mass and Mixing

[This section presents the three neutrino mass-mixing matrix. We also present the full oscillation probability for $\nu_\mu \rightarrow \nu_e$. Simplify it just showing what the parameters are. We define the mixing angle and the phase delta. Includes the mass splitting figure. Conclusion – introduce the idea that $\sin^2 2\theta_{13}$ must be measureable to the level of ~0.01 to proceed to experimentally determine mass hierarchy or delta via this method (accelerator super-beam)]

The two flavor oscillation probability adequately describes neutrino oscillations at the solar and atmospheric Δm^2, however, we know that there are three neutrino flavors and mass states.

The three neutrino mass and flavor states are related by a 3×3 unitary matrix, U :

$$\begin{pmatrix} \nu_e \\ \nu_\mu \\ \nu_\tau \end{pmatrix} = \begin{pmatrix} U_{e1} & U_{e2} & U_{e3} \\ U_{\mu 1} & U_{\mu 2} & U_{\mu 3} \\ U_{\tau 1} & U_{\tau 2} & U_{\tau 3} \end{pmatrix} \begin{pmatrix} \nu_1 \\ \nu_2 \\ \nu_3 \end{pmatrix}$$

where U is defined by convention, with three mixing angles, θ_{12}, θ_{23}, θ_{13} and a phase δ, such that

$$U = \begin{pmatrix} \cos\theta_{12}\cos\theta_{13} & \sin\theta_{12}\cos\theta_{13} & \sin\theta_{13}e^{-i\delta} \\ -\cos\theta_{23}\sin\theta_{12} - \sin\theta_{13}\sin\theta_{23}\cos\theta_{12}e^{i\delta} & \cos\theta_{23}\cos\theta_{12} - \sin\theta_{13}\sin\theta_{23}\sin\theta_{12}e^{i\delta} & \sin\theta_{23}\cos\theta_{13} \\ \sin\theta_{23}\sin\theta_{12} - \sin\theta_{13}\cos\theta_{23}\cos\theta_{12}e^{i\delta} & -\sin\theta_{23}\cos\theta_{12} - \sin\theta_{13}\cos\theta_{23}\sin\theta_{12}e^{i\delta} & \cos\theta_{23}\cos\theta_{13} \end{pmatrix}$$

Neutrino masses are known to be very small, as must be the differences between the masses (unlike in the case of the charged leptons). However, the absolute value of the neutrino mass scale is unknown as is the hierarchical ordering of the mass states – though it has been determined from the solar neutrino data that $m_1 < m_2$ [ref]. What needs to be distinguished are the two possibilities :

$$m_1 < m_2 < m_3$$

from

$$m_3 < m_1 < m_2$$

The first situation is called, by convention, the "normal" mass hierarchy (NH), and the later is called the "inverted" hierarchy (IH). Distinguishing these has important implications in distinguishing models of neutrino mass. It is also interesting to note that a consequence of an inverted hierarchy is that it predicts a larger rate for neutrinoless double-beta decay than the normal hierarchy. The predicted rate in the IH is in fact within the reach of the next generation experiments. Figure 3.5 illustrates the concept of mass and mixing for the two arrangements of the hierarchy.

Just as in the two-neutrino case, one can calculate the probability of flavor transitions among the three neutrino flavors, but the equations becomes quite complicated. As an example, and relevant to the goals of LBNE, one can write down the appearance probability for $\nu_\mu \to \nu_e$ in vacuum :

$$P(\nu_\mu \to \nu_e) =$$

[need to add in equations]

The neutrinos, in fact, do not propagate in a vacuum, but rather traverse matter, where the oscillation probability for $\nu_\mu \to \nu_e$ is modified by the presence of the electron density in the earth. This results in what is called the "matter effect" which enhances the oscillation probability for neutrinos and suppress the probability for anti-neutrinos if the mass hierarchy is normal. The effect is opposite in the inverted hierarchy where neutrinos are suppressed and anti-neutrinos are enhanced. The magnitude of this matter effect is governed by the distance the neutrinos travel and their energy. If L is sufficiently long and E sufficiently high, it is possible to distinguish the NH from the IH by measuring the oscillation probabilities for neutrinos and anti-neutrinos. This opportunity is discussed in more detail in Sections 3.4.4 and 3.4.5.

The current knowledge of the three mixing angles and two Δm^2 are summarized in Table 3.?

Δm^2_{12}	$7.59 \pm 0.02 \times 10^{-5} eV^2$
Δm^2_{23}	$2.43 \pm 0.13 \times 10^{-3} eV^2$
$\sin^2 2\theta_{12}$	0.87 ± 0.03
$\sin^2 2\theta_{23}$	> 0.92
$\sin^2 2\theta_{13}$	$< 0.19 \quad (90\%CL)$

Table 3.? [Ref = PDG live]

To date, only an upper limit on the value of the third mixing angle exists. It should be noted that if θ_{13} were identical to 0, there would be no ν_e content in the ν_3 mass state and there would be no CP violation possible in the neutrino sector. Given that the current experimental bounds indicate that θ_{13} is already known to be small relative to the other angles, it presents a priori an experimental challenge.

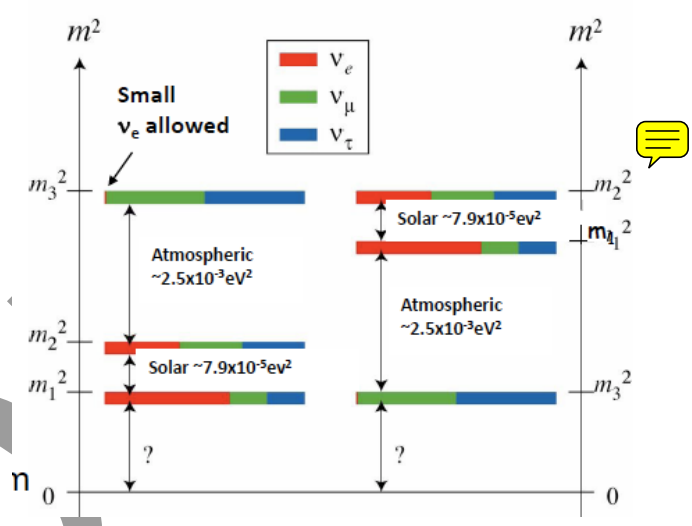

Figure 3.5 Placeholder for a better graphic

3.4.3 Measuring θ_{13}

Two experimentally practical methods exist for measuring θ_{13} using terrestrial sources of neutrinos[6] and efforts on both methods are currently underway. The first approach uses anti-neutrinos from nuclear reactors to search for $\overline{\nu}_e$ disappearance. This is the method which dominates the current limit on θ_{13} from the Chooz reactor experiment [ref]. The current round of experiments under construction include Double Chooz [ref] in France at the same site as the Chooz

[6] It has been suggested that a measurement of θ_{13} might be possible from detection of neutrinos from a galactic supernova burst. Sec discussion in Sections 3.?.

experiment, Daya Bay [ref] in China and Reno [ref] in Korea. Reactor experiments make a ~~clean~~ measurement of $\sin^2 2\theta_{13}$, but have no sensitivity to the CP phase angle, δ, or the mass hierarchy. There are two accelerator-based neutrino beam experiments that will also try to measure θ_{13}. In Japan, the Super-K detector continues to operate and a new neutrino beam from the JPARC accelerator has begun operation. In the U.S., the NOvA experiment will use an upgraded proton source at the Fermilab Main Injector to detect neutrinos from an off-axis component of the NuMI neutrino beam.

The sensitivity of each of these experiments to determining a non-zero value for θ_{13} will increase with exposure time. A summary of this evolution for both discovery and non-observation is shown in Figures 3.? and 3.?. As will be seen from the results presented in Section 3.4.5, a definitive measurement of $\sin^2 2\theta_{13}$ > 0.01 will be a prerequisite for taking the next steps in measuring the oscillation phenomena associated with θ_{13}.

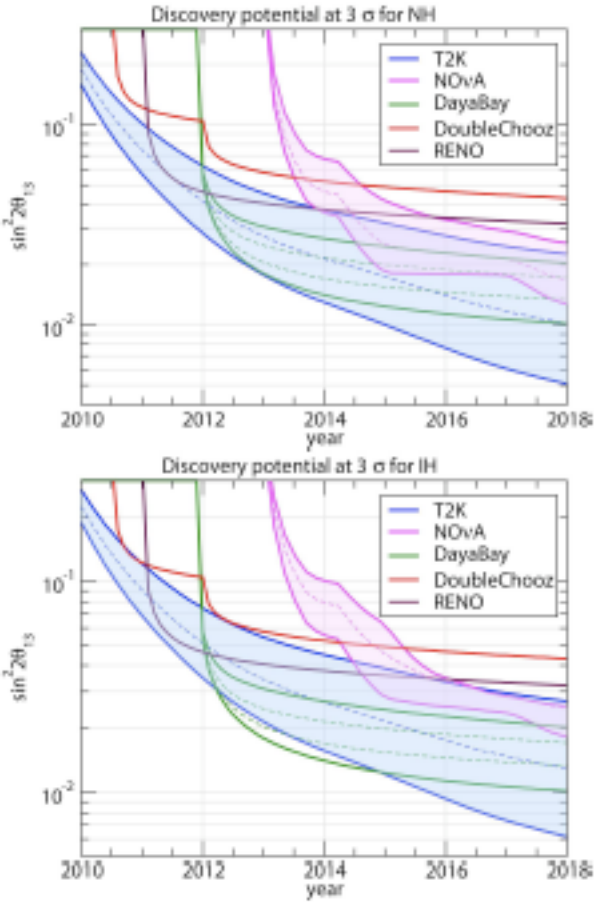

Figure ?? From Reference [] – need permission to use these plots [include caption from text]

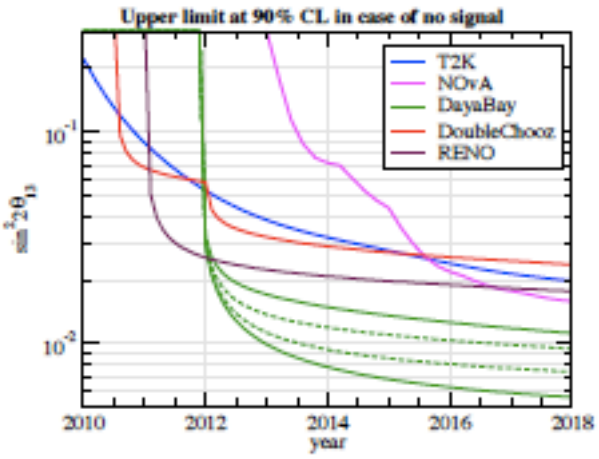

Figure ?? From Reference [] – need permission to use these plots [include caption from text]

3.4.4 Measuring ν_e appearance in LBNE

[In this section, we show the plot of numu2nue probability versus energy for a 1,300-km baseline. We briefly discuss why this is a good choice of baseline. We briefly summarize the characteristics of the neutrino beam and include the reference design spectrum. We include a detailed table of event rates in units of nu/kT/10^20 POT (detector independent-perfect efficiency); use values of sin22theta13 of 0.1(?) and 0.01(?) as extreme limits for the signal. Includes event rates for numu (non oscillated and oscillated), intrinsic and solar nues.]

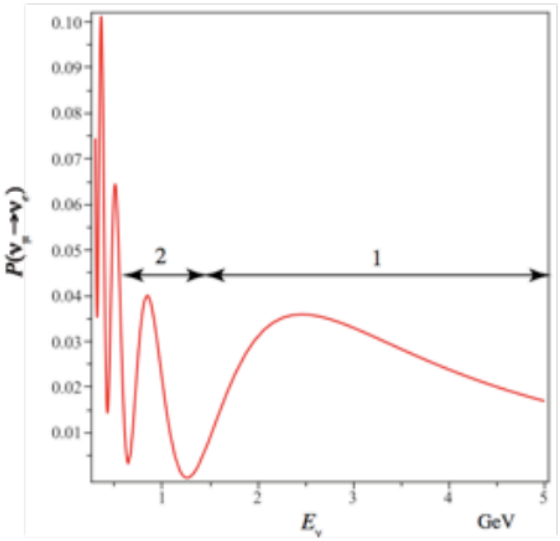

Figure 3.6 Oscillation probability versus neutrino energy for a 1,290-km baseline

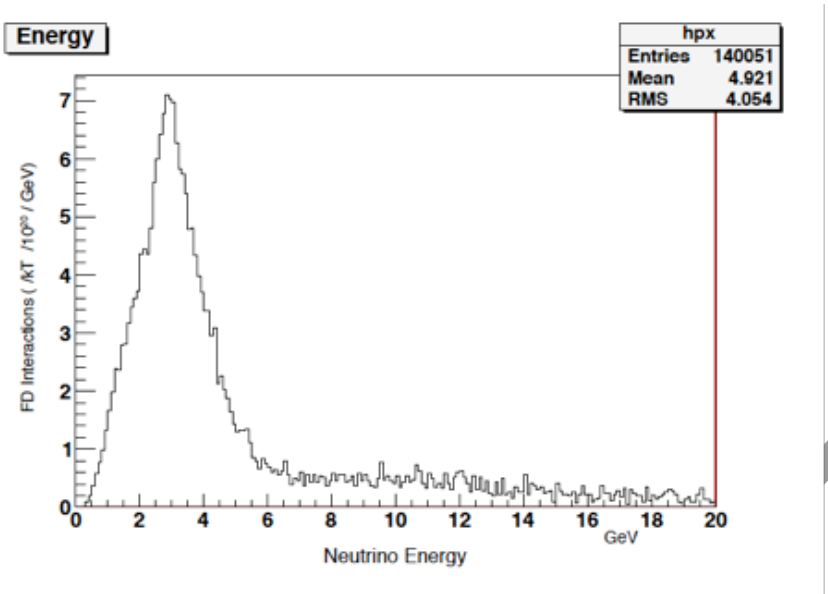

Figure 3.7 : Far detector interactions versus neutrino energy. [Placeholder until we get a final spectrum] The number of charged-current interactions in the absence of oscillations is shown for the reference design. As seen in Fig. 3.6 (above), the significant energy regime for the physics is for energies below 6 GeV. The signal events are a product of this spectrum and the probability of Fig 3.6 (above).

Figure 3.8 PLACEHOLDER for event rates as a function of delta; solid red – normal hierarchy neutrinos; dotted red – inverted hierarchy neutrinos, solid blue- normal hierarchy anti-neutrinos; dotted blue – inverted hierarchy anti-neutrinos

3.4.5 Sensitivity Reach in LBNE

3.4.5.1 θ_{13}, Mass Hierarchy and δ_{CP}

[In this section, we describe how the sensitivity calculations for theta13, mh and CP are done. We present an analysis for a perfect detector, i.e. perfect ν_e efficiency and background only from the intrinsic ν_e in the beam. This analysis determines the perfect detector mass needed to achieve a desired sensitivity for each of the measurements.

The concepts of detector efficiency, background rejection and systematic errors are described and summarized. It tells the reader that the detector designs are what determine these numbers and that **what they are for LBNE are fully described in the respective volumes for each technology and the near detector.**

Sensitivity plots presented in this section are using the parameters of the reference designs presented in the CDR. A table summarizing the performance characteristics of WC and LAr is included (these numbers are generated by the Physics Working Group or detector simulators). All sensitivities are calculated for a number of protons on target (not quoting a beam power).

This section includes a series of sensitivity plots that demonstrate that our reference design configurations are worth building.]

Figures : to be generated

3.4.5.2 Precision Measurements (θ_{23}, Δm^2_{23})

[This section includes the discussion of the precision that can be made on these parameters.]

3.4.6 Oscillation Physics – Conclusion

[Summarize this section with capability as a function of exposure (mass x pot) for the different reference configurations. Conclude with the statement that we wil also be searching for "exotic effects" in neutrino oscillations and other physics beyond the "modified" Standard Model, which now includes massive neutrinos,]

3.5 Search for Proton Decay

3.5.1 Theoretical Motivation and Experimental Status

The search for proton decay tests the observed, but unexplained symmetry of baryon number conservation. The possibility that the proton is unstable has intrigued physicists since the early 1970's when proton decay emerged as a consequence of Grand Unification Theories (GUTs), where one of the most crucial predictions is that the proton must ultimately decay into a lepton and a meson, revealing quark-lepton unity. In Grand Unification Theories the unification of the three forces - strong, electromagnetic and weak, are predicted to occur at an energy scale forever inaccessible at accelerators, ~10^{14} GeV where the decay of a quark into a lepton is mediated by a massive particle, ~~$M_x \sim 10^{14}$ GeV~~ Searches for proton decay are an investigation into that energy regime. This energy scale by definition indicates extremely long lifetimes. Since the dawn of GUT's in the 1970's, the theories have made specific predictions on the preferred modes, branching ratios and lifetimes for the proton. Early theories, i.e. SU(5), predicted numerous decay modes and lifetimes as small as 10^{29} - 10^{30} years. This prompted the first generation searches in the relatively small Soudan, Frejus, Kamiokande and IMB detectors [PDKI]. No signals were observed in these experiments for a large number of decay modes, ruling out the minimal SU(5) theories and opening the door for both new theories and experimental searches.

Following the round of first generation searches, the Superkamiokande detector, became operational in the mid-1990's, and continues to integrate exposure time. Operating through phase I, II, and III, an exposure of 0.17 Megaton years has been accumulated. To date no candidate events have been observed and the best limits have been placed on the $e^+\pi^0$ and $\bar{\nu}K^+$ modes :

$$\frac{\tau}{B(p \to e\pi^0)} > 8 \times 10^{34}\, years$$

$$\frac{\tau}{B(p \to \bar{\nu}K^+)} > 2 \times 10^{33}\, years$$

Figure 3.? illustrates the current state of experimental measurements along with predictions of a number of popular models. An assessment of early 21st century theories shows that numerous and varied models predict proton decay, but lifetime predictions are not precise and typically vary over two or three orders of magnitude. The experimental constraints which now rule out the early theories which predicted relatively short lifetimes lead to the corollary of there being relatively few decay modes, i.e. $e^+\pi^0$, $\overline{\nu}K^+$ and μ^+K^0 .

Experimental searches now need to be prepared to search for very long lifetimes indicating the need for very massive detectors and very long exposure times. GUT theories based on a minimal supersymmetric model predict a unification energy on order of 10^{16} GeV, and push the partial lifetime in the $e^+\pi^0$ channel to order 10^{36} years – more than two orders of magnitude beyond present experimental limits. However, some of these models do predict a partial lifetime of order 10^{34} years in the mode $\overline{\nu}K^+$ which has important implications for a *next* generation search.

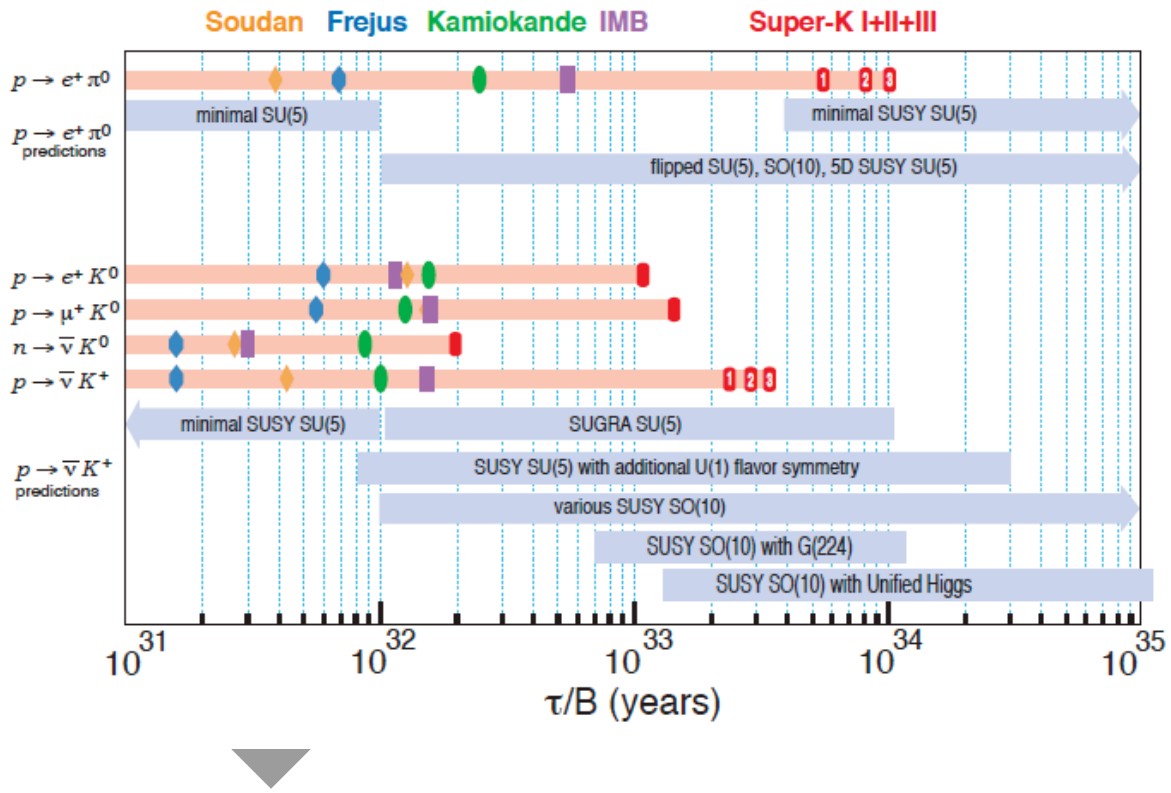

Figure ?? – Reference

3.5.2 Search with LBNE Detectors

[In the following sections, we present the capability of the proposed LBNE detectors to extend the search for proton decay . Include Table summarizing detector performance. Present capability as a function of time for LBNE reference configurations and for increased mass.]

3.5.2.1 $p \rightarrow e^{+}\pi^{0}$

[Describe the signal and what is needed in terms of mass, detector performance, understanding of backgrounds for each detector.]

For both water Cherenkov and liquid argon detectors the mode $p \rightarrow e\pi$ would be fairly easy to distinguish., with similar efficiencies.

Atmospheric neutrino interactions of energy 1 GeV are the most serious background.

3.5.2.2 $p \rightarrow K^{+}\nu$

[Describe the signal and what is needed in terms of mass, detector performance, understanding of backgrounds for the each detector.]

3.5.2.3 Sensitivity versus time

To determine the sensitivity as a function of time, for a given detector mass (or evolution of mass) the needed inputs are : 1) signal detection efficiency, 2) background rate, 3) exposure starting date, 4) detector mass as a function of time and 5) live-time assumptions.

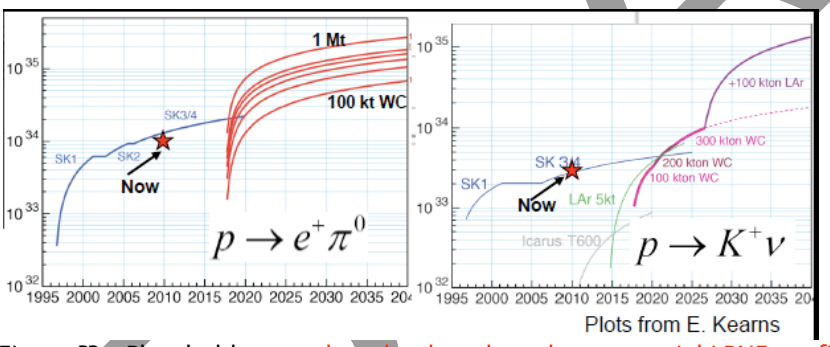

Figure ?? – Placeholder; needs to be done based on potential LBNE configurations

3.5.2.4 Conclusion – Proton Decay

A third generation search undertaken by massive detectors which could become operational in the 2020 era need to compare their potential reach to the integrated exposure that could be achieved by Super-K on the same time scale. Assuming no candidate events are found, by 2020 the Super-K exposure could be approaching 0.5 Mton-years, resulting in a limit on the proton lifetime of $\geq$?$\times 10^{34}$ years. Figure 3.? Shows the evolution of sensitivity, beginning in 2020, for each of the LBNE far detector "reference" configurations. The obvious conclusion from this study is that[…].

There are two potential "game changers" in the search for proton decay that need to be considered. The first is a discovery of SUSY particles at the LHC. This would provide extremely strong motivation to search with high efficiency for the modes involving kaons, in particular $\bar{\nu}K^+$. The second significant occurrence would be the emergence of candidate events in Super-K. This would clearly motivate a confirmation in a larger detector.

[Conclude strongly that the most important detector parameter is mass.]

3.6 Galactic Supernova Bursts

3.6.1 Introduction

A core-collapse supernova will provide a wealth of information via its neutrino signal. About 99% of the supernova's energy is released in an initial neutrino burst that lasts a few tens of seconds, expelling about half the neutrinos in the first second. Due to the small neutrino cross section, we can only detect these massive neutrino bursts from supernovae in our own galaxy or nearby galaxies. Supernova neutrino energies range in the few tens of MeV, and their luminosity is divided more-or-less equally among the ~~three neutrino flavors.~~ The following science topics could be addressed by observing a high-statistics core-collapse neutrino signal:

- The properties of neutrinos : In particular, neutrino oscillations in the core can provide information on oscillation parameters, mass hierarchy and θ_{13}, possibly down to very small values (which will be inaccessible to conventional accelerator experiments), provided that systematics of the supernova models are well understood.

- The astrophysics of core collapse : The time, energy and flavor distribution of the detected neutrinos will give valuable information on the explosion mechanism, accretion, neutron star cooling and possible transitions to ~~quark matter~~ or to a black hole.

- The supernova progenitor : Because the neutrinos emerge promptly after core collapse, in contrast to the electromagnetic radiation which must beat its way out of the stellar envelope, an observed neutrino signal can provide a prompt supernova alert. This could allow astronomers to find the supernova in early light turn-on stages, which may yield information about the progenitor.

3.6.2 Historical Context

The observation of 19 neutrino events in two water Cherenkov detectors for SN1987A in the large Magellanic Cloud (55 kpc) confirmed the baseline model of core collapse, but left many questions unanswered. [Expand and references.]

3.6.3 Predictions

Scientists expect supernovae to occur within or nearby the Milky Way a few times per century. Those at a distance of 10 – 15 kpc have the highest probability of being detected. Within about one Mpc, the rate could be as high as one per year. A distribution of expected event rate versus distance is given in Reference [], and included as Figure []. From 10 kpc (the center of our galaxy), a core-collapse supernova would produce a few hundred neutrino interactions per kiloton of either a water Cherenkov or liquid argon detector. The expected number of events scales with distance as $1/D^2$.

3.6.4 Next Generation Detection

In the following sections, we describe the experimental signatures of supernova neutrinos in the detectors proposed for LBNE, namely water Cherenkov and liquid argon. These two technologies are highly complementary for the detection of supernova neutrinos. A water Cherenkov detector detects $\bar{\nu}_e$, while liquid argon detects mainly ν_e events. A combination of the two would allow important checks on our understanding of astrophysics as well as neutrino properties.

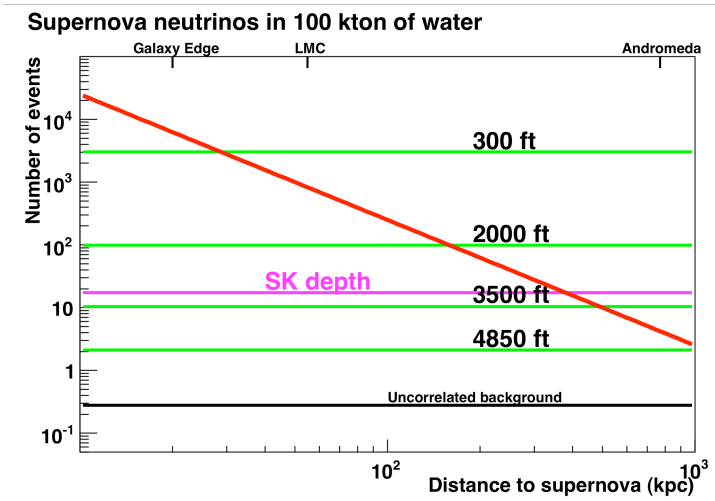

Figure ?? Update – take off the SuperK line ; highlight the LBNE depth(s)

3.6.4.1 Water Cherenkov Detector

In water, the dominant neutrino interaction is the inverse beta decay:

$$\bar{\nu}_e + p \rightarrow e^+ + n \qquad \text{(Eq)}$$

There will also be some charged current (CC) interactions with oxygen in water:

$$\nu_e + {}^{16,18}O \rightarrow {}^{16,18}F + e^-$$
$$\bar{\nu}_e + {}^{16}O \rightarrow {}^{16}N + e^+$$

A cascade of 5-10 MeV de-excitation γ's will also tag:

$$\nu_x + {}^{16}O \rightarrow \nu_x \, {}^{12}O^*$$

Elastic scattering, $\nu_{e,x} + e^- \rightarrow \nu_{e,x} + e^-$, while representing only a few percent of the total signal due to its directional nature, will allow pointing to the supernova. Estimated event rates for the 10-kpc signal in a 100-kT detector are listed in Table 1. [Need to discuss detection efficiency and backgrounds.]

Process	No. of Interactions
$\bar{\nu}_e + p \rightarrow e^+ + n$	23,000
$\nu_e + {}^{16,18}O \rightarrow {}^{16,18}F + e^-$	1,000
$\nu_x + {}^{16}O \rightarrow \nu_x \, {}^{12}O^*$	1,100
$\nu_{e,x} + e^- \rightarrow \nu_{e,x} + e^-$	1,000

Table XX

At the 4,850-ft depth, cosmic ray muon background during the burst should be small in a water detector, even without muon veto rejection. Un-vetoed background in water may come from radioactivity, flashing phototubes, remaining spallation events, or "invisible muons" from atmospheric neutrinos and solar neutrinos, however, these should be negligible in a short-burst time window.

3.6.4.2 Liquid Argon Detector

[Describe the detection mechanism, expected event rates (as a function of distance?) and backgrounds.]

3.7 Supernova Relic Neutrinos

3.7.1 Introduction

Core-collapse supernova explosions throughout the history of the universe left behind a diffuse background of neutrinos, which should be detectable on Earth. While these supernova relic neutrinos (SRN) undoubtedly permeate the universe, they have thus far evaded detection. The flux and spectrum of these neutrinos contain information about the rate of supernova explosions (and consequently the star formation rate) in the past. Because the existence of such a flux is a robust prediction of most models of stellar formation, observation of this flux would provide a key indication that our general idea of how and in what epoch stars formed is correct. Though valuable information can be obtained from a nearby supernova burst, that is a very rare event and one may

not be detected within the next few decades, so that detection of the relic neutrinos is especially important.

To date, Super-Kamiokande has set the world's best limit on the flux of these particles. [Short summary of the results; possibly a table.]

This limit is tantalizingly close to the majority of modern theoretical predictions. Figure [] shows the existing limit on the flux of SRN from Super-Kamiokande and the predictions from several published models.

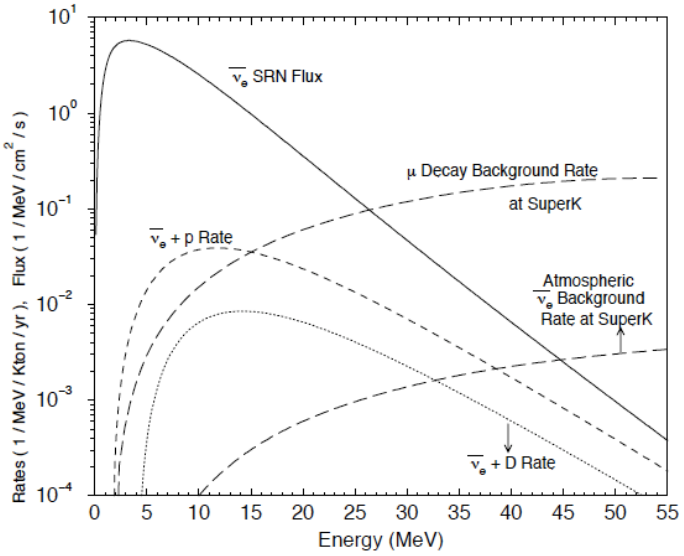

Figure []

Though SRN models vary, according to one widely accepted modern analysis [ref], a 300-kT water Cherenkov detector located deep underground and doped with gadolinium should record about 50 of these supernova events every year. This data would undoubtedly stimulate new theoretical (and perhaps even experimental) developments in the neutrino and cosmology communities.

3.7.2 Detection Requirements and Capability

3.7.2.1 Water Cherenkov Detector

The best signal of supernova relic neutrinos in a water Cherenkov detector is the positrons resulting from the inverse beta reaction (Eq). While the maximum flux occurs at energies below 5 MeV, 10 MeV marks the practical lower limit for detecting positrons from this interaction. This is above the background from reactors (~10 MeV) and well below the atmosphere antineutrino background (~100 MeV). Above ~20 MeV, the dominant background is due to the decay of sub-Cherenkov threshold muons from atmospheric neutrino interactions. This background could be greatly reduced by tagging the neutron that accompanies each inverse beta reaction by observing the γ rays associated with its capture.

[Description of Gd doping gains.]

[For a water Cherenkov detector, we estimate a possible positron energy threshold of 15.5 MeV. For a 300-kT detector located at a depth of 4,850 ft, this will yield a 90% CL sensitivity for the relic neutrino flux of < 0.3 cm-2sec-1, below the predictions in []. This analysis needs to be updated for LBNE detectors constructed in one or two 100-kT modules.]

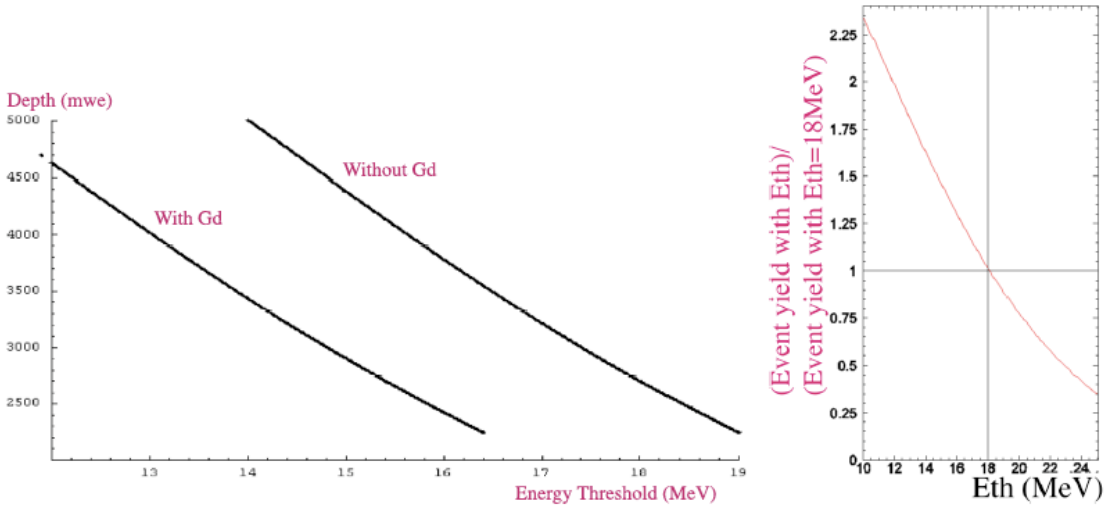

Figure 3.? Placeholder for a plot relevant to LBNE detectors. Not as a function of depth – since that is given.

3.7.2.2 Liquid Argon Detector

Supernova relic neutrinos and antineutrinos will interact in liquid argon detectors via both charged and neutral current interactions.

3.8 Physics with the Near Detector

3.8.1 Measurements for Neutrino Oscillation Physics

[In this section, we discuss the requirements of the near detector to provide the data necessary for the beam oscillation measurements. We summarize the reference design being presented in Volume 3.

3.8.2 Additional Short-baseline Physics

[A brief summary of the additional measurements that could be made with the reference Near Detectors.]

3.9 Additional Physics Opportunities

[The discussion in these sections will depend on the contributions from the Physics Working Groups in these topical areas. Each group should contribute a discussion of the motivation for the measurements and then present the capability to make measurements given the LBNE Project reference detectors. Discussion of results achievable with a different (more desirable, i.e. larger, more PMTs, …) detector can also be submitted and will be included with the appropriate caveats.]

3.9.1 Atmospheric Neutrinos

Atmospheric neutrinos are generated in the upper atmosphere in a uniform spherical thin shell around the Earth. For any detector located at modest depth within the Earth, the flux of neutrinos is isotropic to a good approximation. The detection and study of atmospheric neutrinos has resulted in the remarkable discovery that the muon type neutrinos that come from below the detector over a long distance are suppressed by a factor of ~2 compared to muon neutrinos that come from above the detector. The increase in statistics with larger detectors has beeen matched by the greater accuracy of simulations of the atmospheric flus. For a future large detector, the same study will continue, but will require better control of systematics that could arise from detector geometry, calibrations, backgrounds and electronics. The cosmic ray muon background is important for all of these issues.

[Need input from Physics Working Group]

3.9.2 Solar Neutrinos

[Need introduction and input from Physics Working Group]

3.9.3 Geoneutrinos and Reactor Neutrinos

[Need introduction and input from Physics Working Group]

3.9.4 Ultra High Energy Neutrinos

[Need introduction and input from Physics Working Group]

References

[IMB] IMB

[Kk] Kamiokande

[BP] Pontecorvo 1957 reference

[BK] "On the Quantum Mechanics of Neutrino Oscillations", Boris Kayser, 1981

[SK] Super-Kamiokande Collaboration, S. Fukuda *et al*, Phys. Rev. Lett. **81**, 1562 (1998); S. Fukuda *et al*, Phys. Rev. Lett. **82**, 2644 (1999)

[depth] "Report on the Depth Requirements for a Massive Detector at Homestake", Fermilab TM-2424, BNL-81896-2008

[SNO] SNO Collaboration, Q.R. Ahmad et al, Phys. Rev. Lett. 87, 071301 (2001), Phys. Rev. Lett. **89**, 011301 (2002), Phys. Rev. Lett. **89**, 011302 (2001)

[KL]

[K2K]

[MINOS]

[OPERA]